

CHEMICALLY INDUCED NANOSCALE JOSEPHSON EFFECTS IN NON-STOICHIOMETRIC HIGH- T_c SUPERCONDUCTORS

SERGEI SERGEENKOV^{a,b}

^aCentro de Física das Interações Fundamentais,
Instituto Superior Técnico, Lisboa, Portugal

^bBogoliubov Laboratory of Theoretical Physics,
Joint Institute for Nuclear Research, Dubna, Russia

1. INTRODUCTION

Both granular superconductors and artificially prepared arrays of Josephson junctions (JJAs) proved useful in studying the numerous quantum (charging) effects in these interesting systems, including blockade of Cooper pair tunneling [1], Bloch oscillations [2], propagation of quantum ballistic vortices [3], spin-tunneling related effects using specially designed *SFS*-type junctions [4, 5], novel Coulomb effects in *SINIS*-type nanoscale junctions [6], dynamical AC reentrance [7] and geometric quantization phenomena [8] in 2D JJAs (see, e.g., Ref. [9] for the recent review on charge and spin effects in mesoscopic 2D Josephson junctions).

More recently, it was realized that JJAs can be also used as quantum channels to transfer quantum information between distant sites [10, 11, 12] through the implementation of the so-called superconducting qubits which take advantage of both charge and phase degrees of freedom (see, e.g., Ref. [13] for a review on quantum-state engineering with Josephson-junction devices).

Recent imaging of the granular structure in underdoped $Bi_2Sr_2CaCu_2O_{8+\delta}$ crystals [14], revealed an apparent segregation of its electronic structure into superconducting domains (of the order of a few nanometers) located in an electronically distinct background. In particular, it was found that at low levels of hole doping ($\delta < 0.2$), the holes become concentrated at certain hole-rich domains. Tunneling between such domains leads to intrinsic granular superconductivity (GS) in high- T_c superconductors (HTS). Probably one of the first examples of GS was observed in $YBa_2Cu_3O_{7-\delta}$ single crystals in the form of the so-called "fishtail" anomaly of magnetization [15]. The granular behavior has been related to the 2D clusters of oxygen defects forming twin boundaries (TBs) or dislocation walls within CuO plane that restrict supercurrent flow and allow excess flux to enter the crystal. Indeed, there are serious arguments to consider the TB in HTS as insulating regions of the Josephson SIS-type structure. An average distance between boundaries is essentially less than the grain size. In particu-

lar, the networks of localized grain boundary dislocations with the spacing ranged from $10nm$ to $100nm$ have been observed [15] which produce effectively continuous normal or insulating barriers at the grain boundaries. It was also verified that the processes of the oxygen ordering in HTS leads to the continuous change of the lattice period along TB with the change of the oxygen content. Besides, a destruction of bulk superconductivity in these non-stoichiometric materials with increasing the oxygen deficiency parameter δ was found to follow a classical percolation theory [16].

In addition to their importance for understanding the underlying microscopic mechanisms governing HTS materials, the above experiments can provide rather versatile tools for designing chemically-controlled atomic scale Josephson junctions (JJs) and their arrays (JJAs) with pre-selected properties needed for manufacturing the modern quantum devices [10, 17]. Moreover, as we shall see below, GS based phenomena can shed some light on the origin and evolution of the so-called paramagnetic Meissner effect (PME) which manifests itself both in high- T_c and conventional superconductors [18, 19] and is usually associated with the presence of π -junctions and/or unconventional (d -wave) pairing symmetry.

This Chapter reviews some of the recently suggested novel effects which are expected to occur in intrinsically granular non-stoichiometric material modeled by 2D JJAs which are created by a regular 2D network of twin-boundary (TB) dislocations with strain fields acting as an insulating barrier between hole-rich domains in underdoped crystals. In Section 2 we consider phase-related magnetization effects, including Josephson chemomagnetism (chemically induced magnetic moment in zero applied magnetic field) and its influence on a low-field magnetization (chemically induced PME), and magnetoconcentration effect (creation of extra oxygen vacancies in applied magnetic field) and its influence on a high-field magnetization (chemically induced analog of "fishtail" anomaly). Section 3 addresses charge-related phenomena which are actually dual to the chemomagnetic effects described in Section 2. More specifically, we discuss a possible existence of a non-zero electric polarization (chemomagnetolectric effect) and the related change of the charge balance in intrinsically granular non-stoichiometric material under the influence of an applied magnetic field. In particular, we predict an anomalous low-field magnetic behavior of the effective junction charge and concomitant magnetocapacitance in paramagnetic Meissner phase and a charge analog of "fishtail"-like anomaly at high magnetic fields as well as field-dependent weakening of the chemically-induced Coulomb blockade.

2. CHEMOMAGNETISM AND FISHTAIL ANOMALY

As is well-known, the presence of a homogeneous chemical potential μ through a single JJ leads to the AC Josephson effect with time dependent phase difference $\partial\phi/\partial t = \mu/\hbar$. In this paper, we will consider some effects in dislocation induced JJ caused by a local variation of excess hole concentration $c(\mathbf{x})$ under the chemical pressure (described by inhomogeneous chemical potential $\mu(\mathbf{x})$) equivalent to presence of the strain field of 2D dislocation array $\epsilon(\mathbf{x})$ forming this Josephson contact.

To understand how GS manifests itself in non-stoichiometric crystals, let us invoke an analogy with the previously discussed dislocation models of twinning-induced superconductivity [20] and grain-boundary Josephson junctions [21]. Recall that under plastic deformation, grain boundaries (GBs) (which are the natural sources of weak links in HTS), move rather rapidly via the movement of the grain boundary dislocations (GBDs) comprising these GBs. Using the above evidence, in the previous paper [21] we studied numerous piezomagnetic effects in granular superconductors under mechanical loading. At the same time, observed [14, 15, 22, 23, 24] in HTS single crystals regular 2D dislocation networks of oxygen depleted regions (generated by the dissociation of $\langle 110 \rangle$ twinning dislocations) with the size d_0 of a few Burgers vectors, forming a triangular lattice with a spacing $d \geq d_0$ ranging from $10nm$ to $100nm$, can provide quite a realistic possibility for existence of 2D Josephson network within CuO plane. Recall furthermore that in a d -wave orthorhombic $YBCO$ crystal TBs are represented by tetragonal regions (in which all dislocations are equally spaced by d_0 and have the same Burgers vector \mathbf{a} parallel to y -axis within CuO plane) which produce screened strain fields [23] $\epsilon(\mathbf{x}) = \epsilon_0 e^{-|\mathbf{x}|/d_0}$ with $|\mathbf{x}| = \sqrt{x^2 + y^2}$.

Though in $YBa_2Cu_3O_{7-\delta}$ the ordinary oxygen diffusion $D = D_0 e^{-U_d/k_B T}$ is extremely slow even near T_c (due to a rather high value of the activation energy U_d in these materials, typically $U_d \simeq 1eV$), in underdoped crystals (with oxygen-induced dislocations) there is a real possibility to facilitate oxygen transport via the so-called osmotic (pumping) mechanism [25, 26] which relates a local value of the chemical potential (chemical pressure) $\mu(\mathbf{x}) = \mu(0) + \nabla\mu \cdot \mathbf{x}$ with a local concentration of point defects as follows $c(\mathbf{x}) = e^{-\mu(\mathbf{x})/k_B T}$. Indeed, when in such a crystal there exists a nonequilibrium concentration of vacancies, dislocation is moved for atomic distance a by adding excess vacancies to the extraplane edge. The produced work is simply equal to the chemical potential of added vacancies. What is important, this mechanism allows us to explicitly incorporate the oxygen deficiency parameter δ into our model by relating it to the excess oxygen concentration of vacancies $c_v \equiv c(0)$ as follows $\delta = 1 - c_v$. As a result, the chemical potential of the single vacancy reads $\mu_v \equiv \mu(0) = -k_B T \log(1 - \delta) \simeq k_B T \delta$. Remarkably, the same osmotic mechanism was used by Gurevich and Pashitskii [23] to discuss the modification of oxygen vacancies concentration in the presence of the TB strain field. In particular, they argue that the change of $\epsilon(\mathbf{x})$ under an applied or chemically induced pressure results in a significant oxygen redistribution producing a highly inhomogeneous filamentary structure of oxygen-deficient nonsuperconducting regions along GB [24] (for underdoped superconductors, the vacancies tend to concentrate in the regions of compressed material). Hence, assuming the following connection between the variation of mechanical and chemical properties of planar defects, namely $\mu(\mathbf{x}) = K\Omega_0\epsilon(\mathbf{x})$ (where Ω_0 is an effective atomic volume of the vacancy and K is the bulk elastic modulus), we can study the properties of TB induced JJs under intrinsic chemical pressure $\nabla\mu$ (created by the variation of the oxygen doping parameter δ). More specifically, a single SIS type junction (comprising a Josephson network) is formed around TB due to a local depression of the superconducting order parameter $\Delta(\mathbf{x}) \propto \epsilon(\mathbf{x})$ over distance d_0 producing thus a weak link with (oxygen deficiency δ dependent) Josephson coupling

$J(\delta) = \epsilon(\mathbf{x})J_0 = J_0(\delta)e^{-|\mathbf{x}|/d_0}$ where $J_0(\delta) = \epsilon_0 J_0 = (\mu_v/K\Omega_0)J_0$ (here $J_0 \propto \Delta_0/R_n$ with R_n being a resistance of the junction). Thus, the considered here model indeed describes chemically induced GS in underdoped systems (with $\delta \neq 0$) because, in accordance with the observations, for stoichiometric situation (when $\delta \simeq 0$), the Josephson coupling $J(\delta) \simeq 0$ and the system loses its explicitly granular signature.

To adequately describe chemomagnetic properties of an intrinsically granular superconductor, we employ a model of 2D overdamped Josephson junction array which is based on the well known Hamiltonian

$$\mathcal{H} = \sum_{ij}^N J_{ij}(1 - \cos \phi_{ij}) + \sum_{ij}^N \frac{q_i q_j}{C_{ij}} \quad (1)$$

and introduces a short-range interaction between N junctions (which are formed around oxygen-rich superconducting areas with phases $\phi_i(t)$), arranged in a two-dimensional (2D) lattice with coordinates $\mathbf{x}_i = (x_i, y_i)$. The areas are separated by oxygen-poor insulating boundaries (created by TB strain fields $\epsilon(\mathbf{x}_{ij})$) producing a short-range Josephson coupling $J_{ij} = J_0(\delta)e^{-|\mathbf{x}_{ij}|/d}$. Thus, typically for granular superconductors, the Josephson energy of the array varies exponentially with the distance $\mathbf{x}_{ij} = \mathbf{x}_i - \mathbf{x}_j$ between neighboring junctions (with d being an average junction size). As usual, the second term in the rhs of Eq.(1) accounts for Coulomb effects where $q_i = -2en_i$ is the junction charge with n_i being the pair number operator. Naturally, the same strain fields $\epsilon(\mathbf{x}_{ij})$ will be responsible for dielectric properties of oxygen-depleted regions as well via the δ -dependent capacitance tensor $C_{ij}(\delta) = C[\epsilon(\mathbf{x}_{ij})]$.

If, in addition to the chemical pressure $\nabla\mu(\mathbf{x}) = K\Omega_0\nabla\epsilon(\mathbf{x})$, the network of superconducting grains is under the influence of an applied frustrating magnetic field \mathbf{B} , the total phase difference through the contact reads

$$\phi_{ij}(t) = \phi_{ij}^0 + \frac{\pi w}{\Phi_0}(\mathbf{x}_{ij} \wedge \mathbf{n}_{ij}) \cdot \mathbf{B} + \frac{\nabla\mu \cdot \mathbf{x}_{ij}t}{\hbar}, \quad (2)$$

where ϕ_{ij}^0 is the initial phase difference (see below), $\mathbf{n}_{ij} = \mathbf{X}_{ij}/|\mathbf{X}_{ij}|$ with $\mathbf{X}_{ij} = (\mathbf{x}_i + \mathbf{x}_j)/2$, and $w = 2\lambda_L(T) + l$ with λ_L being the London penetration depth of superconducting area and l an insulator thickness (which, within the discussed here scenario, is simply equal to the TB thickness [26]).

To neglect the influence of the self-field effects in a real material, the corresponding Josephson penetration length $\lambda_J = \sqrt{\Phi_0/2\pi\mu_0 j_c w}$ must be larger than the junction size d . Here j_c is the critical current density of superconducting (hole-rich) area. As we shall see below, this condition is rather well satisfied for HTS single crystals.

Within our scenario, the sheet magnetization \mathbf{M} of 2D granular superconductor is defined via the average Josephson energy of the array

$$\langle \mathcal{H} \rangle = \int_0^\tau \frac{dt}{\tau} \int \frac{d^2x}{s} \mathcal{H}(\mathbf{x}, t) \quad (3)$$

as follows

$$\mathbf{M}(\mathbf{B}, \delta) \equiv -\frac{\partial \langle \mathcal{H} \rangle}{\partial \mathbf{B}}, \quad (4)$$

where $s = 2\pi d^2$ is properly defined normalization area, τ is a characteristic Josephson time, and we made a usual substitution $\frac{1}{N} \sum_{ij} A_{ij}(t) \rightarrow \frac{1}{s} \int d^2x A(\mathbf{x}, t)$ valid in the long-wavelength approximation [27].

To capture the very essence of the superconducting analog of the chemomagnetic effect, in what follows we assume for simplicity that a *stoichiometric sample* (with $\delta \simeq 0$) does not possess any spontaneous magnetization at zero magnetic field (that is $M(0, 0) = 0$) and that its Meissner response to a small applied field B is purely diamagnetic (that is $M(B, 0) \simeq -B$). According to Eq.(4), this condition implies $\phi_{ij}^0 = 2\pi m$ for the initial phase difference with $m = 0, \pm 1, \pm 2, \dots$

Taking the applied magnetic field along the c -axis (and normal to the CuO plane), that is $\mathbf{B} = (0, 0, B)$, we obtain finally

$$M(B, \delta) = -M_0(\delta) \frac{b - b_\mu}{(1 + b^2)(1 + (b - b_\mu)^2)} \quad (5)$$

for the chemically-induced sheet magnetization of the 2D Josephson network.

Here $M_0(\delta) = J_0(\delta)/B_0$ with $J_0(\delta)$ defined earlier (in what follows, $M_0(0)$ is $M_0(\delta \simeq 0)$), $b = B/B_0$, and $b_\mu = B_\mu/B_0 \simeq (k_B T \tau / \hbar) \delta$ where $B_\mu(\delta) = (\mu_v \tau / \hbar) B_0$ is the chemically-induced contribution (which disappears in optimally doped systems with $\delta \simeq 0$), and $B_0 = \Phi_0 / wd$ is a characteristic Josephson field. Fig.1 shows changes of the initial (stoichiometric) diamagnetic magnetization M/M_0 (solid line) with oxygen deficiency δ . As is seen, even relatively small values of δ parameter render a low field Meissner phase strongly paramagnetic (dotted and dashed lines). The inset of Fig.1 presents a true *chemomagnetic* effect with concentration (deficiency) induced magnetization $M(0, \delta)$ in zero magnetic field. According to Eq.(5), the initially diamagnetic Meissner effect turns paramagnetic as soon as the chemomagnetic contribution $B_\mu(\delta)$ exceeds an applied magnetic field B . To see whether this can actually happen in a real material, let us estimate a magnitude of the chemomagnetic field B_μ . Typically [15, 23], for HTS single crystals $\lambda_L(0) \approx 150nm$ and $d \simeq 10nm$, leading to $B_0 \simeq 0.5T$. Using $\tau \simeq \hbar / \mu_v$ and $j_c = 10^{10} A/m^2$ as a pertinent characteristic time and the typical value of the critical current density, respectively, we arrive at the following estimate of the chemomagnetic field $B_\mu(\delta) \simeq 0.5B_0$ for $\delta = 0.05$. Thus, the predicted chemically induced PME should be observable for applied magnetic fields $B \simeq 0.5B_0 \simeq 0.25T$ (which are actually much higher than the fields needed to observe the previously discussed [21] piezomagnetism and stress induced PME in high- T_c ceramics). Notice that for the above set of parameters, the Josephson length $\lambda_J \simeq 1\mu m$, which means that the assumed in this paper small-junction approximation (with $d \ll \lambda_J$) is valid and the so-called "self-field" effects can be safely neglected. So far, we neglected a possible field dependence of the chemical potential μ_v of oxygen vacancies. However, in high enough applied magnetic fields B , the field-induced change of the chemical potential $\Delta\mu_v(B) \equiv \mu_v(B) - \mu_v(0)$ becomes tangible and should be taken into account. As is well-known [28, 29], in a superconducting state $\Delta\mu_v(B) = -M(B)B/n$, where $M(B)$ is the corresponding magnetization, and n is the relevant carriers number density. At the same time, within our scenario, the chemical potential of a single oxygen vacancy μ_v depends on the concentration of oxygen vacancies (through deficiency parameter δ). As a result, two different

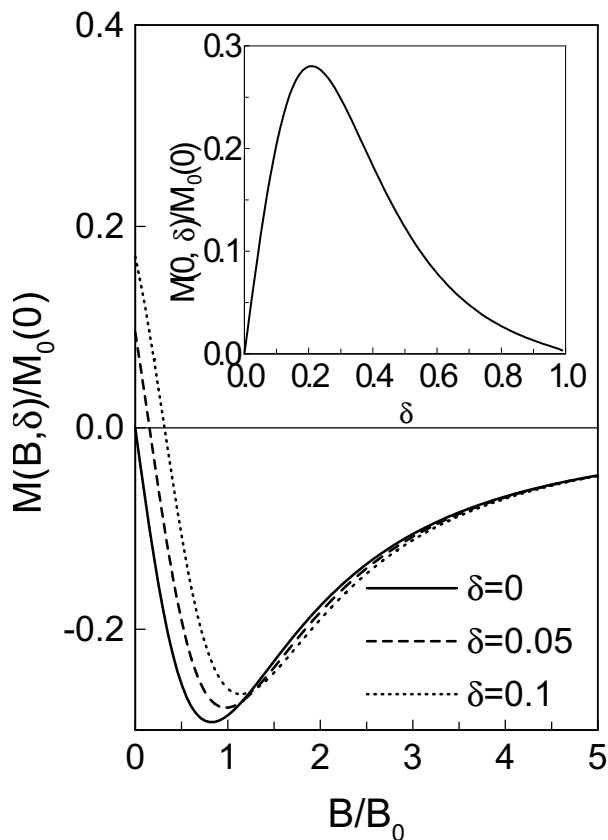


Figure 1: The magnetization $M(B, \delta)/M_0(0)$ as a function of applied magnetic field B/B_0 , according to Eq.(5), for different values of oxygen deficiency parameter: $\delta \simeq 0$ (solid line), $\delta = 0.05$ (dashed line), and $\delta = 0.1$ (dotted line). Inset: δ induced magnetization $M(0, \delta)/M_0(0)$ in a zero applied magnetic field (chemomagnetism).

effects are possible related respectively to magnetic field dependence of $\mu_v(B)$ and to its dependence on magnetization $\mu_v(M)$. The former is nothing else but a superconducting analog of the so-called *magnetoconcentration* effect (which was predicted and observed in inhomogeneously doped semiconductors [30]) with field-induced creation of oxygen vacancies $c_v(B) = c_v(0) \exp(-\Delta\mu_v(B)/k_B T)$, while the latter (as we shall see in the next Section) results in a "fishtail"-like behavior of the magnetization. Let us start with the magnetoconcentration effect. Figure 2 depicts the predicted field-induced creation of oxygen vacancies $\delta(B) = 1 - c_v(B)$ using the above-obtained magnetization $M(B, \delta)$ (see Fig.1 and Eq.(5)). We also assumed, for simplicity, a complete stoichiometry of the system in a zero magnetic field (with $\delta(0) = 1 - c_v(0) = 0$). Notice that $\delta(B)$ exhibits a maximum at $\delta_c \simeq 0.23$ for applied fields $B = B_0$ (in agreement with the classical percolative behavior observed in non-stoichiometric $YBa_2Cu_3O_{7-\delta}$ samples [15, 16, 24]).

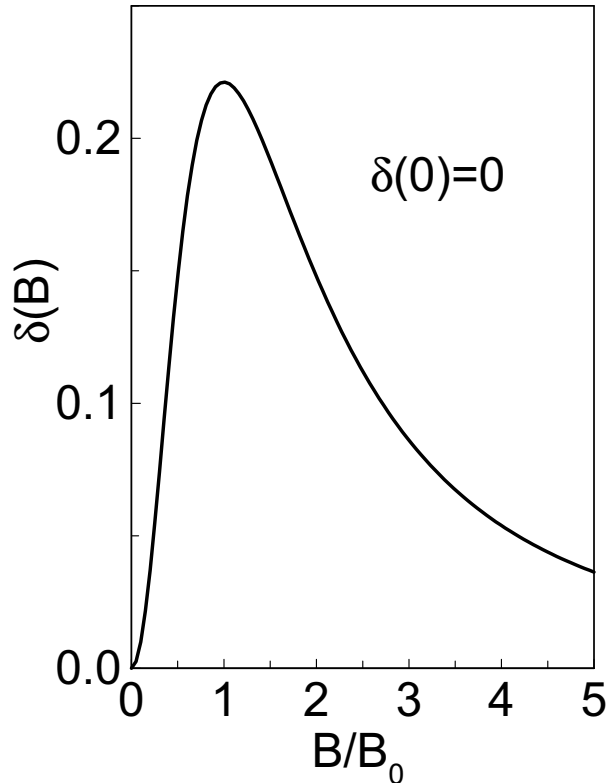


Figure 2: Magnetic field dependence of the oxygen deficiency parameter $\delta(B)$ (magnetoconcentration effect).

Finally, let us show that in underdoped crystals the above-discussed osmotic mechanism of oxygen transport is indeed much more effective than a traditional diffusion. Using typical *YBCO* parameters [23], $\epsilon_0 = 0.01$, $\Omega_0 = a_0^3$ with $a_0 = 0.2nm$, and $K = 115GPa$, we have $\mu_v(0) = \epsilon_0 K \Omega_0 \simeq 1meV$ for a zero-field value of the chemical potential in HTS crystals, which leads to creation of excess vacancies with concentration $c_v(0) = e^{-\mu_v(0)/k_B T} \simeq 0.75$ (equivalent to a deficiency value of $\delta(0) \simeq 0.25$) at $T = T_c$, while the probability of oxygen diffusion in these materials (governed by a rather high activation energy $U_d \simeq 1eV$) is extremely slow under the same conditions because $D \propto e^{-U_d/k_B T_c} \ll 1$. On the other hand, the change of the chemical potential in applied magnetic field can reach as much as [29] $\Delta\mu_v(B) \simeq 0.5meV$ for $B = 0.5T$, which is quite comparable with the above-mentioned zero-field value of $\mu_v(0)$. Let us turn now to the second effect related to the magnetization dependence of the chemical potential $\mu_v(M(B))$. In this case, in view of Eq.(2), the phase difference will acquire an extra $M(B)$ dependent contribution and as a result the r.h.s. of Eq.(5)

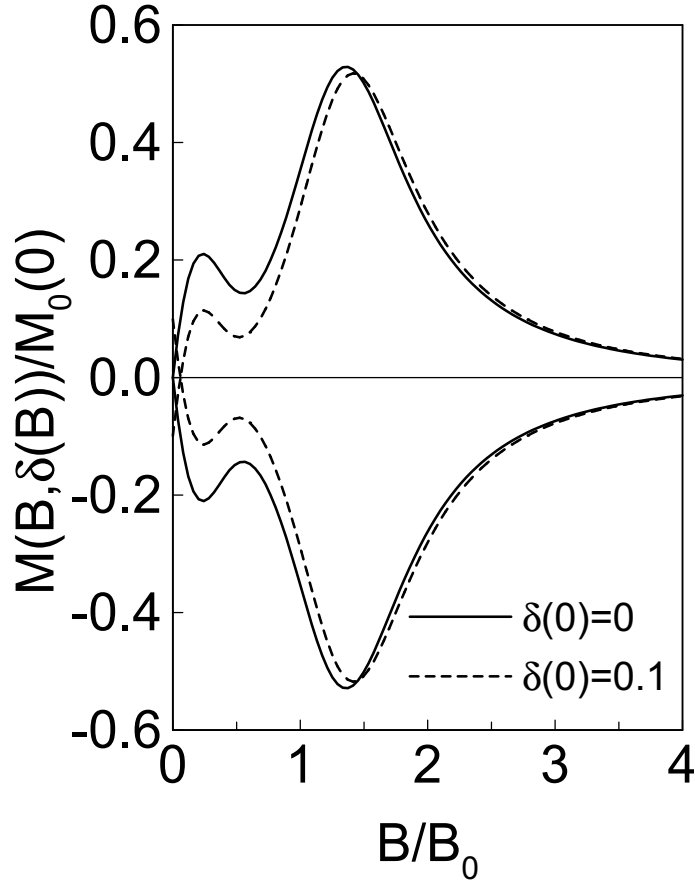


Figure 3: A "fishtail"-like behavior of magnetization $m_f = M(B, \delta(B))/M_0(0)$ in applied magnetic field B/B_0 in the presence of magnetoconcentration effect (with field-induced oxygen vacancies $\delta(B)$, see Fig.2) for two values of field-free deficiency parameter: $\delta(0) \simeq 0$ (solid line), and $\delta(0) = 0.1$ (dashed line).

will become a nonlinear functional of $M(B)$. The numerical solution of this implicit equation for the resulting magnetization $m_f = M(B, \delta(B))/M_0(0)$ is shown in Fig.3 for the two values of zero-field deficiency parameter $\delta(0)$. As is clearly seen, m_f exhibits a field-induced "fishtail"-like behavior typical for underdoped crystals with intragrain granularity (for symmetry and better visual effect we also plotted $-m_f$ in the same figure). The extra extremum of the magnetization appears when the applied magnetic field B matches an intrinsic chemomagnetic field $B_\mu(\delta(B))$ (which now also depends on B via the above-discussed magnetoconcentration effect). Notice that a "fishtail" structure of m_f manifests itself even at zero values of field-free deficiency parameter $\delta(0)$ (solid line in Fig.3) thus confirming a field-induced nature of intrinsic granularity [14, 15, 22, 23, 24]. At the same time, even a rather small deviation from the zero-field stoichiometry (with $\delta(0) = 0.1$) immediately brings about a paramagnetic

Meissner effect at low magnetic fields. Thus, the present model predicts appearance of two interrelated phenomena, Meissner paramagnetism at low fields and "fishtail" anomaly at high fields. It would be very interesting to verify these predictions experimentally in non-stoichiometric superconductors with pronounced networks of planar defects.

3. MAGNETIC FIELD INDUCED POLARIZATION EFFECTS

In this Section, within the same model of JJAs created by a regular 2D network of twin-boundary (TB) dislocations with strain fields acting as an insulating barrier between hole-rich domains in underdoped crystals, we discuss charge-related effects which are actually dual to the above-described phase-related chemomagnetic effects. More specifically, in what follows, we are interested in the behavior of magnetic field induced electric polarization (chemomagnetoelectricity) in chemically induced GS.

Recall that a conventional (zero-field) pair polarization operator within the model under discussion reads [27, 31]

$$\mathbf{p} = \sum_{i=1}^N q_i \mathbf{x}_i \quad (6)$$

In view of Eqs.(1), (2) and (6), and taking into account a usual "phase-number" commutation relation, $[\phi_i, n_j] = i\delta_{ij}$, it can be shown that the evolution of the pair polarization operator is determined via the equation of motion

$$\frac{d\mathbf{p}}{dt} = \frac{1}{i\hbar} [\mathbf{p}, \mathcal{H}] = \frac{2e}{\hbar} \sum_{ij}^N J_{ij} \sin \phi_{ij}(t) \mathbf{x}_{ij} \quad (7)$$

Resolving the above equation, we arrive at the following net value of the magnetic-field induced longitudinal (along x -axis) electric polarization $P(\delta, \mathbf{B}) \equiv \langle p_x(t) \rangle$ and the corresponding effective junction charge

$$Q(\delta, \mathbf{B}) = \frac{2eJ_0}{\hbar\tau d} \int_0^\tau dt \int_0^t dt' \int \frac{d^2x}{S} \sin \phi(\mathbf{x}, t') x e^{-|\mathbf{x}|/d}, \quad (8)$$

where $S = 2\pi d^2$ is properly defined normalization area, τ is a characteristic time (see Discussion), and we made a usual substitution $\frac{1}{N} \sum_{ij} A_{ij}(t) \rightarrow \frac{1}{S} \int d^2x A(\mathbf{x}, t)$ valid in the long-wavelength approximation [27].

To capture the very essence of the superconducting analog of the chemomagnetoelectric effect, in what follows we assume for simplicity that a *stoichiometric sample* (with $\delta \simeq 0$) does not possess any spontaneous polarization at zero magnetic field, that is $P(0, 0) = 0$. According to Eq.(8), this condition implies $\phi_{ij}^0 = 2\pi m$ for the initial phase difference with $m = 0, \pm 1, \pm 2, \dots$

Taking the applied magnetic field along the c -axis (and normal to the CuO plane), that is $\mathbf{B} = (0, 0, B)$, we obtain finally

$$Q(\delta, B) = Q_0(\delta) \frac{2\tilde{b} + b(1 - \tilde{b}^2)}{(1 + b^2)(1 + \tilde{b}^2)^2} \quad (9)$$

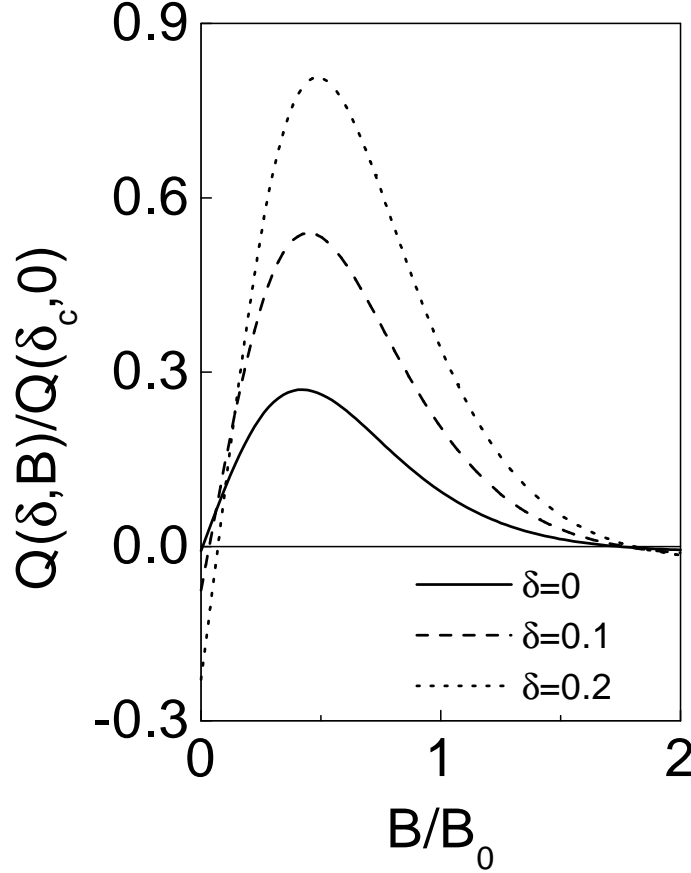


Figure 4: The effective junction charge $Q(\delta, B)/Q(\delta_c, 0)$ (chemomagnetoelectric effect) as a function of applied magnetic field B/B_0 , according to Eq.(9), for different values of oxygen deficiency parameter: $\delta \simeq 0$ (solid line), $\delta = 0.1$ (dashed line), and $\delta = 0.2$ (dotted line).

for the magnetic field behavior of the effective junction charge in chemically induced granular superconductors. Here $Q_0(\delta) = e\tau J_0(\delta)/\hbar$ with $J_0(\delta)$ defined earlier, $b = B/B_0$, $\tilde{b} = b - b_\mu$, and $b_\mu = B_\mu/B_0 \simeq (k_B T \tau / \hbar) \delta$ where $B_\mu(\delta) = (\mu_v \tau / \hbar) B_0$ is the chemically-induced contribution (which disappears in optimally doped systems with $\delta \simeq 0$), and $B_0 = \Phi_0 / wd$ is a characteristic Josephson field.

Fig.4 shows changes of the initial (stoichiometric) effective junction charge Q/Q_0 (solid line) with oxygen deficiency δ . Notice a sign change of Q/Q_0 (dotted and dashed lines) driven by non-zero values of δ at low magnetic fields (a charge analog of chemically induced PME). According to Eq.(9), the effective charge changes its sign as soon as the chemomagnetic contribution $B_\mu(\delta)$ exceeds an applied magnetic field B . At the same time, Fig.5 presents a true *chemoelectric* effect with concentration (deficiency) induced effective junction charge $Q(\delta, 0)$ in zero magnetic field. Notice that $Q(\delta, 0)$ exhibits a maximum around $\delta_c \simeq 0.2$ (in agreement with the classical percolative behavior observed in non-stoichiometric $YBa_2Cu_3O_{7-\delta}$ samples [16]).

It is of interest also to consider the magnetic field behavior of the concomitant

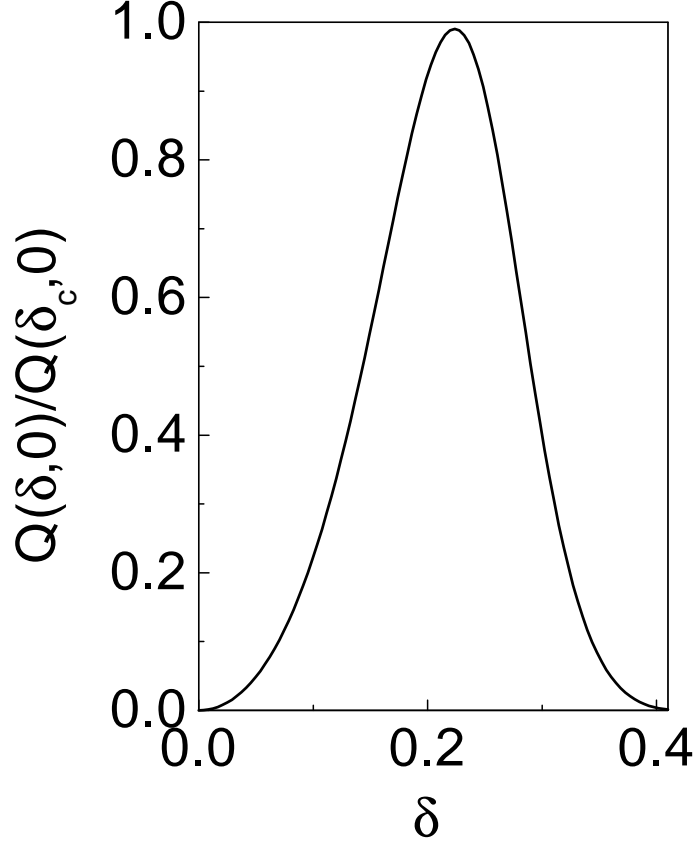


Figure 5: Chemically induced effective junction charge $Q(\delta, 0)/Q(\delta_c, 0)$ in a zero applied magnetic field (true chemoelectric effect).

effective flux capacitance $C \equiv \tau dQ(\delta, B)/d\Phi$ which in view of Eq.(9) reads

$$C(\delta, B) = C_0(\delta) \frac{1 - 3b\tilde{b} - 3\tilde{b}^2 + b\tilde{b}^3}{(1 + b^2)(1 + \tilde{b}^2)^3}, \quad (10)$$

where $\Phi = SB$, and $C_0(\delta) = \tau Q_0(\delta)/\Phi_0$.

Fig.6 depicts the behavior of the effective flux capacitance $C(\delta, B)/C_0(0)$ in applied magnetic field for different values of oxygen deficiency parameter: $\delta \simeq 0$ (solid line), $\delta = 0.1$ (dashed line), and $\delta = 0.2$ (dotted line). Notice a decrease of magnetocapacitance amplitude and its peak shifting with increase of δ and sign change at low magnetic fields which is another manifestation of the charge analog of chemically induced PME (Cf. Fig.4). Up to now, we neglected a possible field dependence of the chemical potential μ_v of oxygen vacancies. Recall, however, that in high enough applied magnetic fields B , the field-induced change of the chemical potential $\Delta\mu_v(B) \equiv \mu_v(B) - \mu_v(0)$ becomes tangible and should be taken into account [28, 29, 32]. As a result, we end up with a superconducting analog of the so-called *magnetoconcentration* effect [32] with field induced creation of oxygen vacancies $c_v(B) = c_v(0) \exp(-\Delta\mu_v(B)/k_B T)$ which in turn brings about a "fishtail"-like behavior of the high-field chemomagnetization (see Section 2 for more details). Fig.7 shows the field behavior of the effective junction

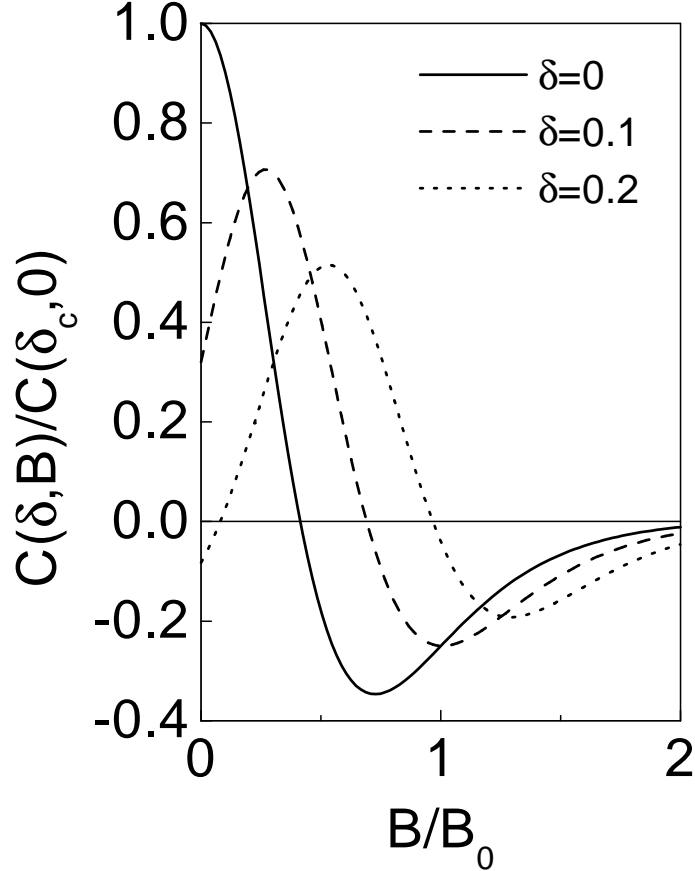


Figure 6: The effective flux capacitance $C(\delta, B)/C(\delta_c, 0)$ as a function of applied magnetic field B/B_0 , according to Eq.(10), for different values of oxygen deficiency parameter: $\delta \simeq 0$ (solid line), $\delta = 0.1$ (dashed line), and $\delta = 0.2$ (dotted line).

charge in the presence of the above-mentioned magnetoconcentration effect. As it is clearly seen, $Q(\delta(B), B)$ exhibits a "fishtail"-like anomaly typical for previously discussed [32] chemomagnetization in underdoped crystals with intragrain granularity (for symmetry and better visual effect we also plotted $-Q(\delta(B), B)$ in the same figure). This more complex structure of the effective charge appears when the applied magnetic field B matches an intrinsic chemomagnetic field $B_\mu(\delta(B))$ (which now also depends on B via the magnetoconcentration effect). Notice that a "fishtail" structure of $Q(\delta(B), B)$ manifests itself even at zero values of field-free deficiency parameter $\delta(0)$ (solid line in Fig.7) thus confirming a field-induced nature of intrinsic granularity. Likewise, Fig.8 depicts the evolution of the effective flux capacitance $C(\delta(B), B)/C_0(0)$ in applied magnetic field B/B_0 in the presence of magnetoconcentration effect (Cf. Fig.6). Thus, the present model predicts appearance of two interrelated phenomena dual to the previously discussed behavior of chemomagnetism (see Section 2), namely a charge analog of Meissner paramagnetism at low fields and a charge analog of "fishtail" anomaly at high fields. To see whether these effects can be actually observed in a real material, let us estimate an order of magnitude of the main model parameters.

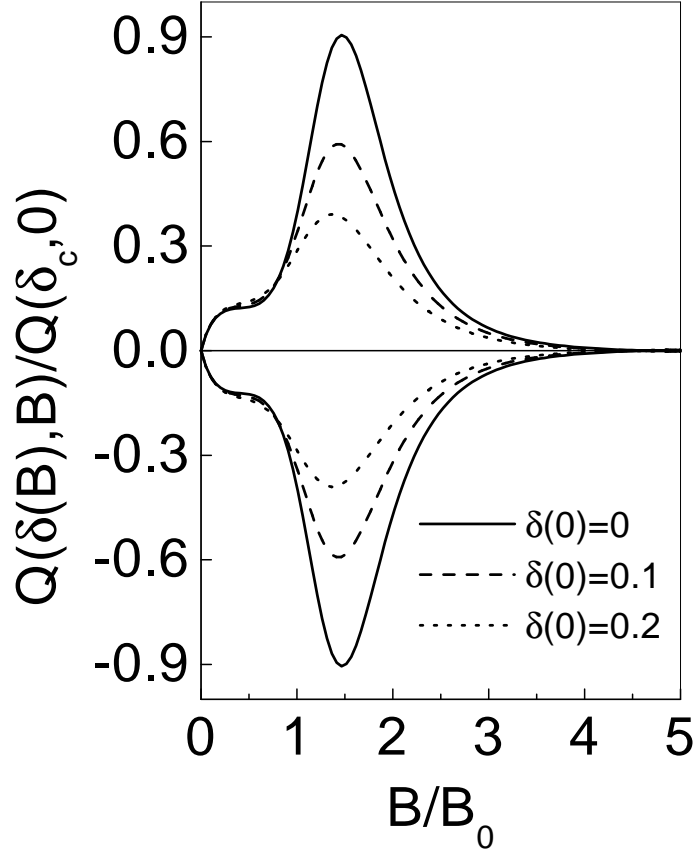


Figure 7: A "fishtail"-like behavior of effective charge $Q(\delta(B), B)/Q(\delta_c, 0)$ in applied magnetic field B/B_0 in the presence of magnetoconcentration effect (with field-induced oxygen vacancies $\delta(B)$) for three values of field-free deficiency parameter: $\delta(0) \simeq 0$ (solid line), $\delta(0) = 0.1$ (dashed line), and $\delta(0) = 0.2$ (dotted line).

Using typical for HTS single crystals values of $\lambda_L(0) \simeq 150nm$, $d \simeq 10nm$, and $j_c \simeq 10^{10}A/m^2$, we arrive at the following estimates of the characteristic $B_0 \simeq 0.5T$ and chemomagnetic $B_\mu(\delta) \simeq 0.5B_0$ fields, respectively. So, the predicted charge analog of PME should be observable for applied magnetic fields $B < 0.25T$. Notice that, for the above set of parameters, the Josephson length is of the order of $\lambda_J \simeq 1\mu m$, which means that the assumed in this paper small-junction approximation is valid and the "self-field" effects can be safely neglected.

Furthermore, the characteristic frequencies $\omega \simeq \tau^{-1}$ needed to probe the suggested here effects are related to the processes governed by tunneling relaxation times $\tau \simeq \hbar/J_0(\delta)$. Since for oxygen deficiency parameter $\delta = 0.1$ the chemically-induced zero-temperature Josephson energy in non-stoichiometric *YBCO* single crystals is of the order of $J_0(\delta) \simeq k_B T_C \delta \simeq 1meV$, we arrive at the required frequencies of $\omega \simeq 10^{13}Hz$ and at the following estimates of the effective junction charge $Q_0 \simeq e = 1.6 \times 10^{-19}C$ and flux capacitance $C_0 \simeq 10^{-18}F$. Notice that the above estimates fall into the range of parameters used in typical experiments for studying the single-electron tunneling effects

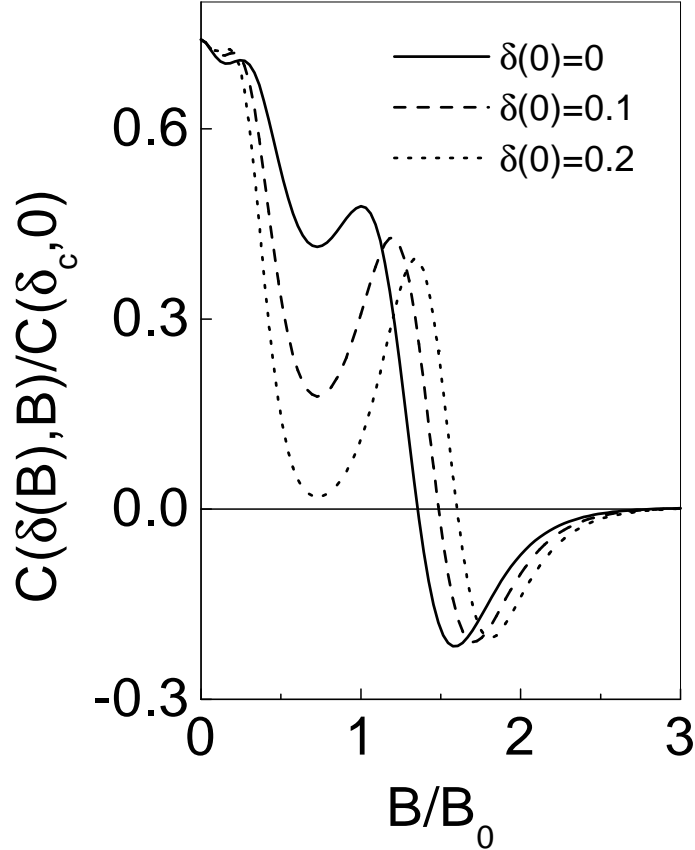


Figure 8: The behavior of the effective flux capacitance $C(\delta(B), B)/C(\delta_c, 0)$ in applied magnetic field B/B_0 in the presence of magnetoconcentration effect for three values of field-free deficiency parameter: $\delta(0) \simeq 0$ (solid line), $\delta(0) = 0.1$ (dashed line), and $\delta(0) = 0.2$ (dotted line).

both in JJs and JJAs [1, 2, 13, 33] suggesting thus quite an optimistic possibility to observe the above-predicted field induced effects experimentally in non-stoichiometric superconductors with pronounced networks of planar defects or in artificially prepared JJAs. (It is worth mentioning that a somewhat similar behavior of the magnetic field induced charge and related flux capacitance has been observed in 2D electron systems [34].)

And finally, it can be easily verified that, in view of Eqs.(6)-(8), the field-induced Coulomb energy of the oxygen-depleted region within our model is given by

$$E_C(\delta, B) \equiv \left\langle \sum_{ij}^N \frac{q_i q_j}{2C_{ij}} \right\rangle = \frac{Q^2(\delta, B)}{2C(\delta, B)} \quad (11)$$

with $Q(\delta, B)$ and $C(\delta, B)$ defined by Eqs. (9) and (10), respectively.

A thorough analysis of the above expression reveals that in the PME state (when $B \ll B_\mu$) the chemically-induced granular superconductor is in the so-called Coulomb blockade regime (with $E_C > J_0$), while in the "fishtail" state (for $B \geq B_\mu$) the energy balance tips in favor of tunneling (with $E_C < J_0$). In particular, we obtain that

$E_C(\delta, B = 0.1B_\mu) = \frac{\pi}{2}J_0(\delta)$ and $E_C(\delta, B = B_\mu) = \frac{\pi}{8}J_0(\delta)$. It would be also interesting to check this phenomenon of field-induced weakening of the Coulomb blockade experimentally.

4. CONCLUSION

In conclusion, within a realistic model of 2D Josephson junction arrays (created by 2D network of twin boundary dislocations with strain fields acting as an insulating barrier between hole-rich domains in underdoped crystals), a few novel effects expected to occur in intrinsically granular material are predicted, including phase-related and (dual) charge-related phenomena. The conditions under which these effects can be experimentally measured in non-stoichiometric high- T_c superconductors were discussed.

ACKNOWLEDGMENTS

This work was done during my stay at the Center for Physics of Fundamental Interactions (Instituto Superior Técnico, Lisbon) and was partially funded by the FCT. I thank Pedro Sacramento and Vitor Vieira for hospitality and interesting discussions on the subject. I am also indebted to Anant Narlikar for his invitation to make this contribution for the Special Golden Jubilee volume of the Studies.

References

- [1] M. Iansity, A.J. Johnson, C.J. Lobb et al., Phys. Rev. Lett. **60** (1988) 2414
- [2] D.B. Haviland, L.S. Kuzmin, P. Delsing et al., Z. Phys. B **85** (1991) 339
- [3] H.S.J. van der Zant, Physica B **222** (1996) 344
- [4] V.V. Ryazanov, V.A. Oboznov, A.Yu. Rusanov et al., Phys. Rev. Lett. **86** (2001) 2427
- [5] A.A. Golubov, M.Yu. Kupriyanov, and Ya.V. Fominov, JETP Lett. **75** (2002) 588
- [6] P.M. Ostrovsky and M.V. Feigel'man, JETP Lett. **79** (2004) 489
- [7] F.M. Araujo-Moreira, P. Barbara, A.B. Cawthorne et al., Phys. Rev. Lett. **78** (1997) 4625; P. Barbara, F.M. Araujo-Moreira, A.B. Cawthorne et al., Phys. Rev. B **60** (1999) 7489; F.M. Araujo-Moreira, W. Maluf, and S. Sergeenkov, Eur. Phys. J. B **44** (2005) 33
- [8] S. Sergeenkov and F.M. Araujo-Moreira, JETP Lett. **80** (2004) 580
- [9] I.V. Krive, S.I. Kulinich, R.I. Shekhter et al., Low Temp. Phys. **30** (2004) 554
- [10] L.B. Ioffe, M.V. Feigel'man, A. Ioselevich et al., Nature **415** (2002) 503

- [11] D. Born, V.I. Shnyrkov, W. Krechet et al., Phys. Rev. B **70** (2004) 180501
- [12] A.B. Zorin, JETP **98** (2004) 1250
- [13] Yu. Makhlin, G. Schön, and A. Shnirman, Rev. Mod. Phys. **73** (2001) 357
- [14] K.M. Lang, V. Madhavan, J.E. Hoffman et al., Nature **415** (2002) 412
- [15] M. Daeumling, J.M. Seuntjens, D.C. Larbalestier et al., Nature **346** (1990) 332; I.M. Babich and G.P. Mikitik, JETP Lett. **64** (1996) 586
- [16] V.F. Gantmakher, A.M. Neminskii, and D.V. Shovkun, JETP Lett. **52** (1990) 630
- [17] S. Sergeenkov, *Studies of High Temperature Superconductors*, v. **39** (Ed. A. Narlikar), Nova Sci. Publishers, NY (2001), pp. 117-131; F.M. Araujo-Moreira, P. Barbara, A.B. Cawthorne, and C.J. Lobb, *Studies of High Temperature Superconductors*, v. **43** (Ed. A. Narlikar), Nova Sci. Publishers, NY (2002), pp. 227-242; S. Sergeenkov, *New Developments in Superconductivity Research* (Ed. R.W. Stevens), Nova Sci. Publishers, NY (2003), pp. 18-45
- [18] V. Kataev, N. Knauf, W. Braunisch et al., JETP Lett. **58** (1993) 636; A.K. Geim, S.V. Dubonos, J.G.S. Lok et al., Nature **396** (1998) 144; M.S. Li, Phys. Rep. **376** (2003) 133
- [19] C. De Leo and G. Rotoli, Phys. Rev. Lett. **89** (2002) 167001
- [20] I. N. Khlyustikov and M. S. Khaikin, JETP **48** (1978) 583; M. S. Khaikin and I. N. Khlyustikov, JETP Lett. **33** (1981) 158
- [21] S. Sergeenkov, JETP Lett. **70** (1999) 36
- [22] G. Yang, P. Shang, S.D. Sutton et al., Phys. Rev. B **48** (1993) 4054
- [23] A. Gurevich and E.A. Pashitskii, Phys. Rev. B **56** (1997) 6213
- [24] B.H. Moeckley, D.K. Lathrop, and R.A. Buhrman, Phys. Rev. B **47** (1993) 400
- [25] L.A. Girifalco, *Statistical Physics of Materials* (A Wiley-Interscience Publication, New York, 1973)
- [26] S. Sergeenkov, J. Appl. Phys. **78** (1995) 1114
- [27] S. Sergeenkov, JETP Lett. **76** (2002) 170
- [28] A.A. Abrikosov, *Fundamentals of the Theory of Metals* (Elsevier, Amsterdam, 1988)
- [29] S. Sergeenkov and M. Ausloos, JETP **89** (1999) 140
- [30] A.A. Akopyan, S.S. Bolgov, A.P. Savchenko et al., Sov. Phys. Semicond. **24** (1990) 1167
- [31] S. Sergeenkov, J. de Physique I (France) **7** (1997) 1175
- [32] S. Sergeenkov, JETP Lett. **77** (2003) 94
- [33] P.J.M. van Bentum, H. van Kempen, L.E.C. van de Leemput et al., Phys. Rev. Lett. **60** (1988) 369
- [34] W. Chen, T.P. Smith, M. Buttiker et al., Phys. Rev. Lett. **73** (1994) 146